Abdominal Imaging

Published online: 18 December 2013

Abdom Imaging (2014) 39:262–268
DOI: 10.1007/s00261-013-0054-0

Coronal reformatted CT images contribute to the precise evaluation of the radiofrequency ablative margin for hepatocellular carcinoma

Tenyu Motoyama,[1] Sadahisa Ogasawara,[1] Tetsuhiro Chiba,[1] Takashi Higashide,[2] Hajime Yokota,[2] Naoya Kanogawa,[1] Eiichiro Suzuki,[1] Yoshihiko Ooka,[1] Akinobu Tawada,[1] Ryosuke Irie,[3] Shigehiro Ochi,[3] Yoshitada Masuda,[3] Takashi Uno,[2] Osamu Yokosuka[1]

[1]Department of Gastroenterology and Nephrology, Graduate School of Medicine, Chiba University, 1-8-1 Inohana, Chuo-ku, Chiba 260-8670, Japan
[2]Department of Radiology, Graduate School of Medicine, Chiba University, Chiba, Japan
[3]Department of Radiology, Chiba University Hospital, Chiba, Japan

Abstract

Objective: The purpose of the present study was to evaluate the usefulness of coronal reformatted images obtained from 64-slice multi-detector computed tomography to assess the ablative margin (AM) in hepatocellular carcinoma (HCC) treated with radio frequency ablation (RFA).
Methods: Ninety-five HCC nodules were analyzed in 66 HCC patients treated with RFA. Two radiologists and one hepatologist independently reviewed axial CT images with or without coronal reformatted images in HCC treated with RFA. Nodules were determined as AM-sufficient (≥5 mm) or AM-insufficient (<5 mm). The level of interobserver agreement was measured using the weighted kappa test. The sensitivity, specificity, and positive and negative predictive values (NPVs) of an insufficient AM (<5 mm) to predict local recurrence were evaluated.
Results: The numbers of AM-sufficient nodules judged by readers 1–3 based on axial images and both axial and coronal images were 56, 49, and 58, and 47, 33, and 48, respectively. Excellent agreement and good to excellent agreement were obtained among the three readers on axial image readings and both axial and coronal image readings, respectively. The mean sensitivity, specificity, and positive and NPVs of an insufficient AM on axial images and both axial and coronal images to predict local recurrence were 64%, 60%, 17%, and 93%, and 95%, 50%, 20%, and 97%, respectively.
Conclusions: Coronal reformatted CT images should be utilized to evaluate the AM in HCC treated with RFA in order to decrease the risk of local recurrence following treatment.

Key words: Hepatocellular carcinoma—Radiofrequency ablation—Ablative margin—Coronal reformation—CT

Hepatocellular carcinoma (HCC) is the fifth most common cancer in the world [1]. Radiofrequency ablation (RFA) is minimally invasive and has been widely applied to the local treatment of HCC. The efficacy of RFA for small HCC was shown to be equal to that of surgical resection in terms of overall survival [2, 3].

Insufficient ablation frequently results in the local recurrence of treated lesions. Therefore, an ablative margin (AM) of at least 5 mm is required to avoid local recurrence in HCC treated with RFA [4]. The AM can be conventionally assessed using axial images of enhanced computed tomography (CT) or magnetic resonance imaging (MRI). In current clinical practice, an evaluation of technical success is based on the visual comparison of pre- and post-RFA CT images using landmarks such as hepatic vessels and the liver surface [5, 6]. However, it is difficult to estimate the presence and

Tenyu Motoyama and Sadahisa Ogasawara contributed equally to this work.

Correspondence to: Tetsuhiro Chiba; *email:* techiba@faculty.chiba-u.jp

extent of the safety margin using only a visual, section-by-section comparison of pre- and post-RFA CT images because changes in a patient's position and respiratory motion have been shown to cause nonlinear motion or deformation in the liver [6]. Several studies have demonstrated the diagnostic usefulness of coronal reformations of 64-slice multi-detector computed tomography (64-MDCT) images detecting HCC [7, 8]. However, whether coronal reformations on 64-MDCT are useful for evaluating the AM of HCC treated with RFA remains unclear.

In the present study, we attempted to assess the utility of coronal reformations of 64-MDCT images in assessing the AM following RFA.

Patients and methods

Study design and patient population

A total of 122 patients with HCC were treated with RFA in our institution between October 2009 and September 2010. Patients with a sufficient follow-up of 2 years were enrolled in this study. Patients treated with not only RFA, but also additional treatments such as transcatheter arterial chemoembolization (TACE) against original tumors were excluded. Among them, patients treated with non-ablative treatments (including TACE) against relapsed lesions in the contralateral hemiliver during the follow-up period were included. A total of 95 HCC nodules were retrospectively analyzed in 66 patients treated with RFA (Fig. 1). These patients had been diagnosed with HCC based on histological examinations or the current AASLD practice guidelines [9]. Informed consent was obtained from all patients. This study was approved by the Ethics Committee of the Graduate School of Medicine, Chiba University.

RFA protocol

Inclusion criteria for percutaneous ablation were as follows: total bilirubin concentration lower than 3 mg/dL; platelet count not less than $50 \times 10^3/mm^3$; and prothrombin activity not lower than 50%. Patients with portal vein tumor thrombosis, refractory ascites, or extrahepatic metastasis were excluded [10]. The RFA procedure has been described elsewhere [11]. Briefly, RFA was performed percutaneously under ultrasound guidance (Power Vision 8000, Aplio XV or Aplio XG; Toshiba, Tokyo, Japan). After the administration of sedatives and local anesthesia, a 17-gage cooled-tip electrode (Cool-Tip; RF Ablation System, Covidien, Boulder, Colombia, CO) was inserted. Radiofrequency energy was delivered for 6–15 min for each application. RFA was performed by five experienced hepatologists (T. M., S. O., T. C., N. K., and A. T.).

CT protocol

CT examinations were performed using a five-phase (precontrast, early arterial, late arterial, portal, equilibrium) technique with the MDCT system (Aquillion One or Aquillion 64; Toshiba Medical, Tokyo, Japan). The slice thickness was 5 mm, and table feed was 5 mm. Each patient was injected with 100 ml of a nonionic contrast material (iopamidol, Iopamiron 370; Bayer Yakuhin, Ltd., Osaka, Japan) at a rate of 3.5 mL/s using a power injector (Nemoto Kyorindo Co., Ltd., Tokyo, Japan). The bolus tracking method was used to scan each patient. The trigger threshold level was set at 200 Hounsfield units (HU) at the level of the descending aorta. CT was performed immediately before the administration of contrast medium and during the early hepatic arterial, late hepatic arterial, and equilibrium phases 5, 20, and

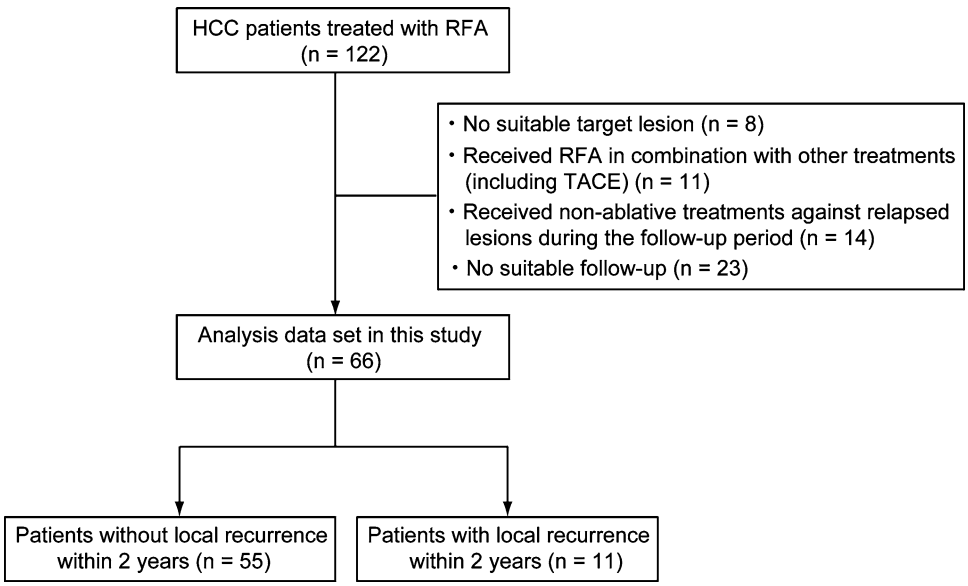

Fig. 1. Flow diagram showing the patients enrolled in this study.

50 s after the trigger, respectively. Images of equilibrium phases were then obtained 150–180 s after the administration of contrast medium.

Assessment of treatment efficacy and follow-up

The efficacy of RFA was assessed with contrast-enhanced CT with a section thickness of 5 mm performed the next day. The complete ablation of HCC was defined as hypoattenuation of the lesion including the surrounding liver parenchyma. Patients received additional sessions of RFA until the treatment was judged as sufficient. Follow-up consisted of monthly blood tests and monitoring of tumor markers at the outpatient clinic, and dynamic CT and ethoxybenzyl diethylenetriamine-enhanced MRI were performed every 3–4 months with a median follow-up period of 24.9 months (range 0–35.0 months). The follow-up periods of patients with or without local recurrence were 8.1 months (range 0–18.0 months) and 28.3 months (range 24.0–35.0 months), respectively. Intrahepatic HCC recurrence was classified as either tumor recurrence at a site distant from the primary tumor or adjacent to the treated site (local tumor progression). A diagnosis of intrahepatic recurrence was made by at least two modalities among CT, MRI, ultrasonography, angiography, and needle tumor biopsy.

Image analysis

Preoperative CT images were independently reviewed by two gastrointestinal radiologists (H.Y and T.H with 8 and 11 years of experience, respectively) and one hepatologist (Y.O with 11 years of experience). Before the present study began, discrepancies in reviews between the three readers were resolved by a discussion to reach a consensus. Each reading session was separated by 4 weeks to minimize recall bias. All images were read on an open-source PACS workstation DICOM viewer (OsiriX 64-bit, ver. 3.7.1). Patient information such as name, gender, age, and hospital record number was removed from the images for blinded readings. We defined ablated surrounding hepatic parenchyma as a low-attenuation rim around a central high attenuation area on post-RFA CT images. To evaluate whether the size of a high attenuation area on pre-RFA CT images agreed with the tumor size, we compared the tumor size on enhanced CT before treatment with the size of the low-attenuation area on post-RFA CT images. Post-RFA HCC nodules with at least a 5-mm distance of a circumferential low attenuation were classified as AM-sufficient (≥5 mm) (Fig. 2A). Nodules were classified as AM-insufficient (<5 mm), if less than 5 mm was observed between the outer margin of the lesion and the circumferential low attenuation in treated lesions (Fig. 2B). When a central high attenuation area was not clearly observed on post-RFA CT images, the AM was determined by a careful comparison between pre-RFA CT images and post-RFA images

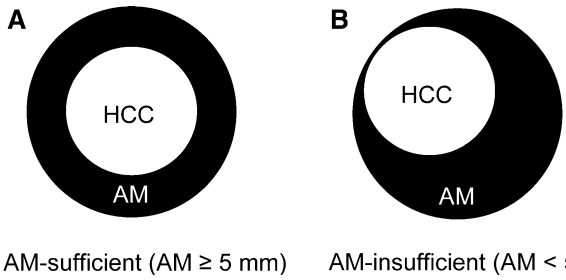

Fig. 2. Classification of the radiofrequency ablative margin by post-RFA CT images. **A** When HCC treated with RFA was surrounded with a low-attenuation rim (LAR, ≥5 mm), the nodule was determined as ablative margin (AM)-sufficient. **B** When HCC treated with RFA was surrounded with a LAR (<5 mm), the nodule was determined as AM-insufficient.

Statistical analysis

Agreement between readers for assessment of the AM based on axial images and both axial and coronal images was determined using the κ statistic. Differences in the average κ value between axial images and both axial and coronal images were assessed by means of the jackknife method. The sensitivity, specificity, and positive and negative predictive values (NPVs) of AM to predict local recurrence were calculated. The Kaplan–Meier method was used to calculate the cumulative rate of local recurrence, and the log-rank test was used for statistical analysis. P values less than 0.05 were considered significant. All statistical analyses were performed using IBM SPSS Statistics 18 (SPSS Japan).

Results

Baseline characteristics of patients and nodules

Forty-three male patients and 23 female patients with an average age of 73 years (59–91 years) participated in this study (Table 1). Liver damage was attributed to HBV (n = 11), HCV (n = 43), both HBV and HCV (n = 2), alcohol abuse (n = 3), and unknown etiology (n = 7). The numbers of patients classified into Child–Pugh A and B were 45 and 21, respectively. The number of patients with 1, 2, 3, and more than 3 nodules was 44, 21, 1, and 0, respectively. Among the 95 nodules analyzed in this study, 2 nodules had diameters less than 10 mm. Pathological examinations prior to RFA revealed that these nodules were composed of moderately differentiated HCC; therefore, they were treated with RFA and included in this study. Only 3 of the 95 HCC nodules examined in 66 patients were larger than 30 mm in diameter.

Table 1. Baseline characteristics of the 66 HCC patients (95 nodules)

Characteristics	
Age (years)	73 (range 59–91)
Gender (male/female)	43/23
Child–Pugh score (*A*/*B*)	45/21
Etiology of liver disease	
Hepatitis B virus	13
Hepatitis C virus	45
Alcohol abuse	3
Tumor number	
1	44
2, 3	21
4≤	1
Tumor size (median, mm)	18 (range 7–33)
Prior treatment (yes/no)	40/26
Local ablation	33
Hepatectomy	2
Others	5
Total bilirubin (median, mg/dL)	1.2 (range 0.5–2.5)
Albumin (median, g/dL)	3.7 (range 2.4–4.8)
Platelet (median, $\times 10^4/\mu L$)	10.7 (range 3.3–27.3)
Alpha-fetoprotein (median, ng/mL)	52 (range 2.5–563.8)
Des-γ-carboxy prothrombin (median, mAU/mL)	52 (range 7–513)

Table 2. Assessment of the AM in HCC treated with RFA

Axial images	Both axial and coronal images		
	AM-sufficient	AM-insufficient	Total
Reader 1			
AM-sufficient	40	16	56
AM-insufficient	7	32	39
Total	47	48	95
Reader 2			
AM-sufficient	30	19	49
AM-insufficient	3	43	46
Total	33	62	95
Reader 3			
AM-sufficient	40	18	58
AM-insufficient	8	29	37
Total	48	47	95

Assessment of the AM by axial images or both axial and coronal images

The AM was estimated by axial images and both axial and coronal images by 3 readers (Table 2). Axial image readings by readers 1–3 showed that the numbers of AM-sufficient nodules were 56, 49, and 58, respectively. Both axial and coronal image readings by readers 1–3 also revealed that the numbers of AM-sufficient nodules were 47, 33, and 48, respectively. On the other hand, axial image readings by readers 1–3 showed that the numbers of AM-insufficient nodules were 39, 46, and 37, respectively. The numbers of AM-insufficient nodules judged by readers 1–3 based on both axial and coronal images were 48, 62, and 47, respectively. Taken together, reading both axial and coronal images clearly showed that the number of AM-sufficient nodules was lower, and the number of AM-insufficient nodules was higher than those from axial image readings only.

Table 3. Agreement between pairs of readers

	κ		
	Reader 1 vs reader 2	Reader 2 vs reader 3	Reader 3 vs reader 1
Axial images	0.80	0.80	0.86
Both axial and coronal images	0.70	0.64	0.81

Inter-reader agreement

Good to excellent agreement (κ range 0.64–0.81) was obtained among the three readers for reading both axial and coronal images, whereas excellent agreement (κ range 0.80–0.86) was obtained among the three readers for reading axial images (Table 3).

Comparison of the AM assessment between axial images and both axial and coronal images

The AM agreement rates between axial images and both axial and coronal images judged by readers 1–3 were 76% (72/95), 77% (73/95), and 73% (69/95), respectively (Fig. 3A–D). Concerning AM-sufficient nodules on axial images judged by readers 1–3, 16 of 56 nodules (29%), 19 of 49 nodules (39%), and 18 of 58 nodules (29%) were determined to be AM-insufficient by reading both axial and coronal images (Fig. 3E–H). Although 39, 46, and 37 nodules were classified as AM-insufficient on axial images by readers 1–3, 7 of 39 nodules (18%), 3 of 46 nodules (7%), and 8 of 37 nodules (22%) were determined to be AM-sufficient by reading both axial and coronal images, respectively.

Investigation of local recurrence after RFA in view of the AM

Local recurrence was observed in 11 nodules in 11 patients during observation periods following RFA in patients with HCC. We then calculated the sensitivity, specificity, and positive and NPVs of an insufficient AM (<5 mm) to predict local recurrence (Table 4). As expected, the sensitivity of an insufficient AM on both axial and coronal images was higher than that on axial images. Conversely, the specificity of an insufficient margin on both axial and coronal image readings was lower than that on axial image readings. Additionally, both axial and coronal image readings modestly improved the positive predictive value (PPV) and NPV.

Only 1 of the 47 and 1 of the 48 AM-sufficient nodules judged by readers 1 and 3 by reading both axial and coronal images showed local recurrence. The nodule was also determined to be AM-sufficient on axial images. No recurrence was found in the 33 nodules classified as AM-sufficient judged by reader 2 by reading both axial and

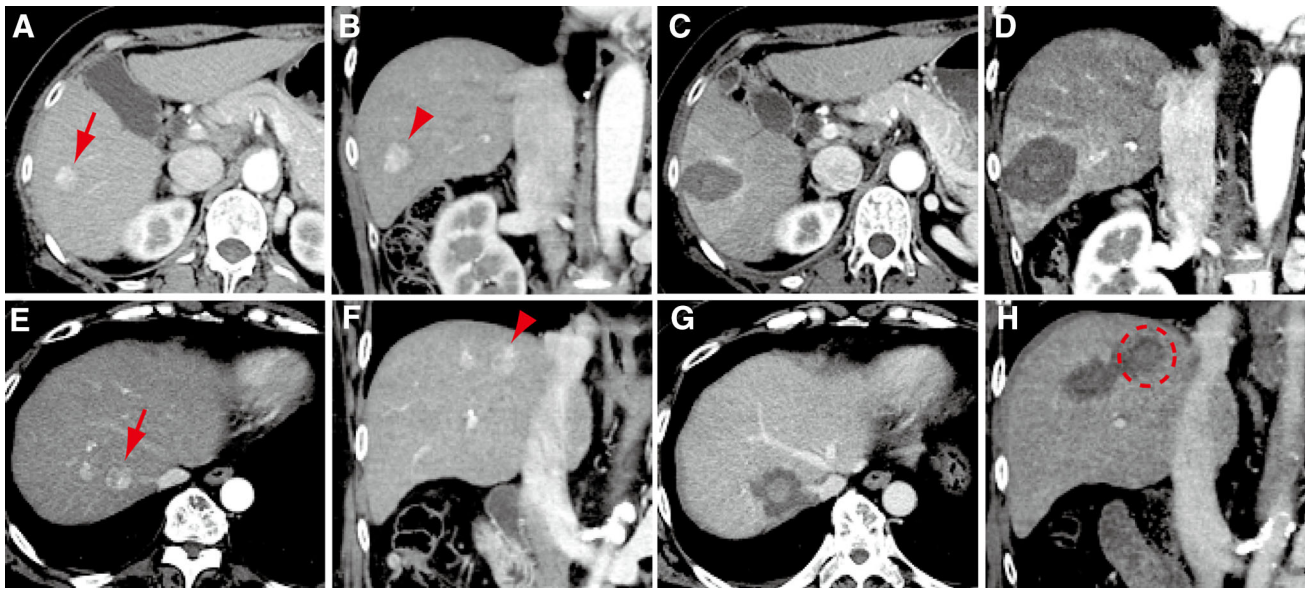

Fig. 3. Representative CT images of pre- and post-RFA. **A–D** A 65-year-old woman with a 17 mm HCC in liver segment V. **A** An axial image of the tumor (*arrows*) in the hepatic arterial phase. **B** A coronal reformatted image of the tumor (*arrowhead*) in the hepatic arterial phase. **C** An axial image of post-RFA. The tumor was evaluated as ablative margin (AM)-sufficient. **D** A coronal reformatted image of post-RFA. The tumor was evaluated as AM-sufficient on axial images. **E–H** A 78-year-old man with a 17 mm HCC in liver segment VII. **E** An axial image of the tumor (*arrows*) in the hepatic arterial phase. **F** A coronal reformatted image of the tumor (*arrowheads*) in the hepatic arterial phase. **G** An axial image of post-RFA. The tumor was evaluated as AM-sufficient. **H** A coronal reformatted image of post-RFA. The ablated lesion (surrounded by a *dotted line*) was evaluated as AM-insufficient as opposed to the result obtained from axial image readings.

Table 4. Sensitivity, specificity, PPV, and NPV of an insufficient AM (<5 mm) to predict local recurrence (95% CI)

	Reader 1 (%)	Reader 2 (%)	Reader 3 (%)	Mean value (%)
Sensitivity				
Axial images	64 (30–89)	64 (31–89)	64 (31–89)	64
Axial and coronal images	91 (59–99)	100 (71–100)	93 (59–99)	95
Specificity				
Axial images	62 (50–72)	54 (42–65)	64 (53–74)	60
Axial and coronal images	55 (44–65)	39 (29–50)	56 (45–67)	50
Positive predictive value				
Axial images	18 (8–34)	15 (6–29)	19 (8–35)	17
Axial and coronal images	21 (11–35)	18 (9–30)	21 (11–35)	20
Negative predictive value				
Axial images	93 (83–98)	92 (80–97)	93 (83–98)	93
Axial and coronal images	98 (88–99)	100 (89–100)	98 (88–99)	99

coronal images. In contrast, local recurrence was observed in 4 of the 56 (7%), 4 of the 49 (8%), and 4 of the 58 AM-sufficient nodules (6%) judged by readers 1–3 by reading axial images, respectively. These nodules were determined to be AM-negative on both axial and coronal images.

To examine the local recurrence of AM-sufficient nodules assessed by readers 1–3 on axial images, we re-divided them into 2 groups (AM-sufficient or AM-insufficient) in view of the AM based on both axial and coronal image readings. The cumulative local recurrence rates were significantly higher in AM-insufficient nodules than in AM-sufficient nodules assessed by both axial and coronal images (Fig. 4A). In AM-insufficient nodules on axial images, no significant differences were observed in the local recurrence rates between AM-sufficient nodules and AM-insufficient nodules assessed by both axial and coronal images (Fig. 4B). Taken together, the evaluation of the AM on both axial and coronal images instead of on axial images only is beneficial for predicting of local recurrence.

Discussion

RFA is a prevailing technology for the local treatment of HCC. Ablation of not only the tumor itself, but also the surrounding liver parenchyma is considered necessary to obtain a sufficient therapeutic response. Therefore,

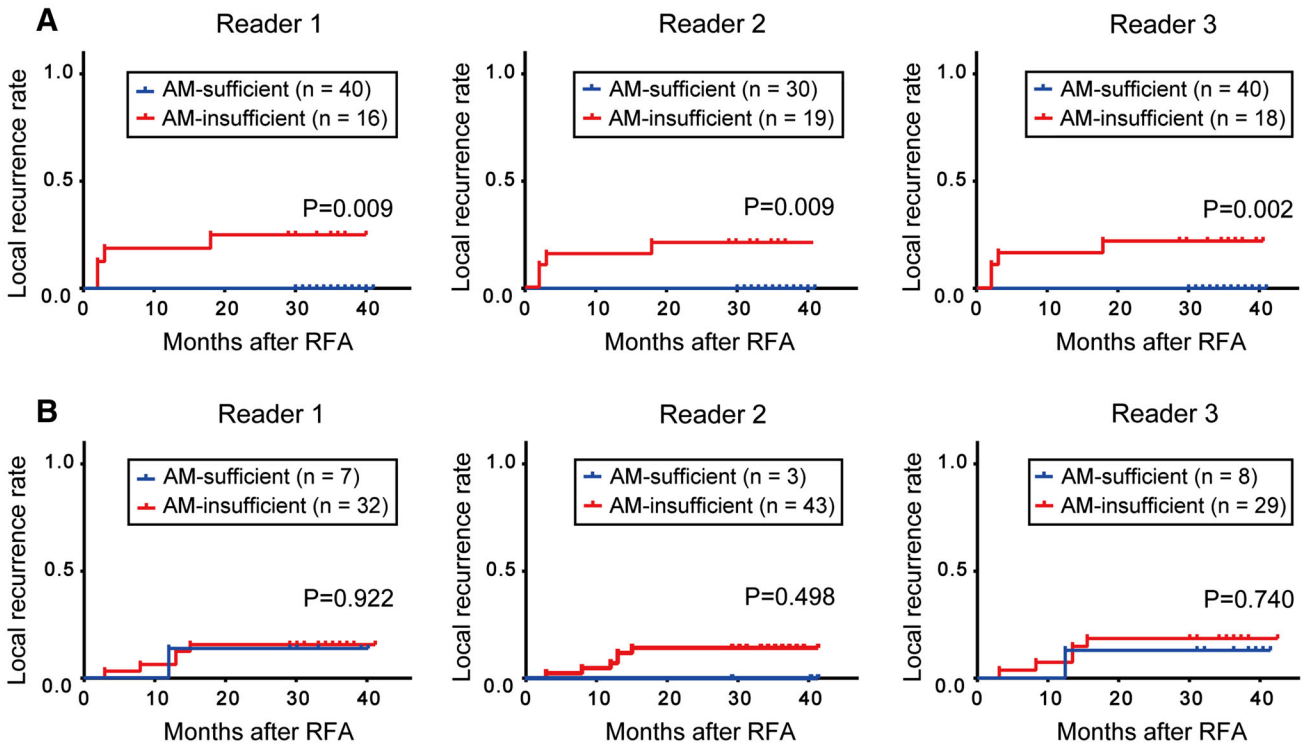

Fig. 4. Comparison of local recurrence rates between AM-sufficient nodules and AM-negative nodules on axial and coronal images. **A** AM-sufficient nodules on axial images were divided into two groups (AM-sufficient or AM-insufficient) based on the findings of both axial and coronal images. **B** AM-insufficient nodules on axial images were divided into two groups (AM-sufficient or AM-insufficient) based on the findings of both axial and coronal images.

evaluating the AM is of paramount importance. Although the AM has typically been assessed by axial images of enhanced CT and MRI, recent studies revealed that other modalities in diagnostic imaging such as super paramagnetic iron oxide (SPIO)-enhanced MRI and contrast-enhanced ultrasonography enabled a more precise evaluation of the AM [12, 13]. Imaging fusion techniques such as the registration of pre-RFA axial CT images onto post-RFA images appear to be useful and accurate for evaluating the AM [14, 15].

Coronal images were previously shown to be able to demonstrate vascular and biliary systems in the liver in the longitudinal axis and provide additional information on the location and extent of HCC. Coronal reformatting techniques have also enabled us to recognize the relationship between tumor and hepatic vasculatures, which is essential for the accurate preoperative planning of RFA. 64-MDCT is recently widely used because of its low cost, short examination time, and wide availability. Coronal reformatted CT images obtained from 64-MDCT have also been shown to be particularly useful in both the detection of tumors and tumor progression in various cancers including HCC [6, 7]. In the present study, we applied the coronal reformation of 64-MDCT images to HCC treated with RFA to evaluate the radiofrequency AM. The results obtained demonstrated that 29–39% of AM-sufficient nodules assessed on axial images were considered to have an insufficient AM by reading both axial and coronal images. In contrast, 7–22% of AM-insufficient nodules assessed on axial images were considered to have a sufficient AM by reading both axial and coronal images. These results indicated that the assessment ability of the AM based on both axial and coronal images was better than that based on axial images.

We then highlighted the discrepancies mentioned above and reanalyzed AM-sufficient nodules assessed by axial images. Kaplan–Meier curves showed that local recurrence rates were significantly higher in AM-insufficient nodules than in AM-sufficient nodules based on both axial and coronal images. We investigated the ability of an insufficient AM to predict local recurrence. As expected, the sensitivity of an insufficient margin to predict local recurrence in both axial and coronal image readings was markedly higher than that in axial image readings. In contrast, the specificity of an insufficient margin in both axial and coronal image readings was lower than that in axial image readings. Because AM-insufficient nodules do not necessarily show local recurrence, the higher sensitivity and lower specificity in both axial and coronal image readings than those in axial image readings are inextricably linked. In addition, modest improvements in both PPV and NPV were observed. Although further studies with longer observation periods and larger numbers of nodules are necessary to

strengthen these findings, it is possible that the combined interpretation of both axial and coronal image sets enabled us to recognize an insufficient AM following RFA. Additional ablation treatment may contribute to a decrease in the local recurrence of RFA-treated lesions. Inter-reader agreement analysis showed decreased agreement when both axial and coronal images were used. To accurately judge the AM, several readers assessing the AM may be more appropriate in daily clinical practice.

Local tumor progression after RFA was previously shown to develop more frequently from the area of the thinnest AM [16]. The site of recurrence was also most commonly observed in the craniocaudal direction [14]. Concordant with this finding, our study showed that local recurrence in the craniocaudal direction and horizontal direction was observed in eight and three nodules, respectively. Taken together, the assessment of the AM in the craniocaudal direction should be carefully performed on both axial and coronal images. Because both sagittal reformatted images and coronal images contribute to a more accurate diagnosis than axial images alone in pulmonary embolism and renal cell carcinoma [17, 18], sagittal image readings may be useful for evaluating the AM in HCC. Further analyses are needed.

In conclusion, coronal reformatted images obtained from 64-MDCT were very useful for evaluating the AM. A set of axial and coronal images should be utilized in patients with HCC treated with RFA to prevent local recurrence after the RFA procedure.

Acknowledgments. The authors thank Dr. Fumihiko Kanai (Medical Corporation Eikenkai) for the valuable discussions.

Conflict of interest. There is no conflict of interest to disclose.

References

1. El-Serag HB, Rudolph KL (2007) Hepatocellular carcinoma: epidemiology and molecular carcinogenesis. Gastroenterology 132:2557–2576
2. Cho YK, Kim JK, Kim MY, et al. (2009) Systematic review of randomized trials for hepatocellular carcinoma treated with percutaneous ablation therapies. Hepatology 49:453–459
3. Garrean S, Hering J, Saied A, et al. (2008) Radiofrequency ablation of primary and metastatic liver tumors: a critical review of the literature. Am J Surg 195:508–520
4. Park MH, Rhim H, Kim YS, et al. (2008) Spectrum of CT findings after radiofrequency ablation of hepatic tumors. Radiographics 28:379–390
5. Barker DW, Zagoria RJ, Morton KA, et al. (2005) Evaluation of liver metastases after radiofrequency ablation: utility of 18F-FDG PET and PET/CT. AJR Am J Roentgenol 184:1096–1102
6. Schraml C, Clasen S, Schwenzer NF, et al. (2008) Diagnostic performance of contrast-enhanced computed tomography in the immediate assessment of radiofrequency ablation success in colorectal liver metastases. Abdom Imaging 33:643–651
7. Yanaga Y, Awai K, Nakaura T, et al. (2008) Optimal contrast dose for depiction of hypervascular hepatocellular carcinoma at dynamic CT using 64-MDCT. AJR Am J Roentgenol 190:1003–1009
8. Marin D, Catalano C, De Filippis G, et al. (2009) Detection of hepatocellular carcinoma in patients with cirrhosis: added value of coronal reformations from isotropic voxels with 64-MDCT. AJR Am J Roentgenol 192:180–187
9. Bruix J, Sherman M (2011) American Association for the Study of Liver Diseases. Management of hepatocellular carcinoma: an update. Hepatology 53:1020–1022
10. Tateishi R, Shiina S, Teratani T, et al. (2005) Percutaneous radiofrequency ablation for hepatocellular carcinoma. An analysis of 1000 cases. Cancer 103:1201–1209
11. Shiina S, Teratani T, Obi S, et al. (2005) A randomized controlled trial of radiofrequency ablation with ethanol injection for small hepatocellular carcinoma. Gastroenterology 129:122–130
12. Tokunaga S, Koda M, Matono T, et al. (2012) Assessment of ablative margin by MRI with ferucarbotran in radiofrequency ablation for liver cancer: comparison with enhanced CT. Br J Radiol 85:745–752
13. Inoue T, Kudo M, Hatanaka K, et al. (2013) Usefulness of contrast-enhanced ultrasonography to evaluate the post-treatment responses of radiofrequency ablation for hepatocellular carcinoma: comparison with dynamic CT. Oncology 84(Suppl 1):51–57
14. Tomonari A, Tsuji K, Yamazaki H, et al. (2013) Feasibility of fused imaging for the evaluation of radiofrequency ablative margin for hepatocellular carcinoma. Hepatol Res 43:728–734
15. Kim KW, Lee JM, Klotz E, et al. (2011) Safety margin assessment after radiofrequency ablation of the liver using registration of preprocedure and postprocedure CT images. AJR Am J Roentgenol 196:W565–W572
16. Koda M, Tokunaga S, Miyoshi K, et al. (2012) Assessment of ablative margin by unenhanced magnetic resonance imaging after radiofrequency ablation for hepatocellular carcinoma. Eur J Radiol 81:2730–2736
17. Lee EY, Zucker EJ, Tsai J, et al. (2011) Pulmonary MDCT angiography: value of multiplanar reformatted images in detecting pulmonary embolism in children. AJR Am J Roentgenol 197:1460–1465
18. Tsili AC, Argyropoulou MI, Gousia A, et al. (2012) Renal cell carcinoma: value of multiphase MDCT with multiplanar reformations in the detection of pseudocapsule. AJR Am J Roentgenol 199:379–386